Ocean biogeochemical fingerprints of fast-sinking tunicate and fish detritus

Jessica Y. Luo[1], Charles A. Stock[1], John P. Dunne[1], Grace K. Saba[2], Lauren Cook[2]

[1]NOAA Ocean and Atmospheric Research, Geophysical Fluid Dynamics Laboratory, 201 Forrestal Rd, Princeton NJ 08540
[2]Center for Ocean Observing Leadership, Department of Marine and Coastal Sciences, School of Environmental and Biological Sciences, Rutgers University, New Brunswick, NJ USA

Manuscript correspondence: Jessica.Luo@noaa.gov

Submitted to Geophysical Research Letters.

ORCiD:
JYL: 0000-0002-0032-9370
CAS: 0000-0001-9549-8013
JPD: 0000-0002-8794-0489
GKS: 0000-0002-3874-895X

Main points:

- We incorporated fast-sinking detritus from pelagic tunicates and fishes into a modified version of the ocean biogeochemical model COBALT.
- The fast-sinking detritus increased carbon sequestration and transfer efficiency to depth, but decreased surface productivity and export.
- Fast-sinking detritus decreased the size of oxygen minimum zones (OMZs) and water column denitrification, a common model bias.

Abstract

Pelagic tunicates (salps, pyrosomes) and fishes generate jelly-falls and/or fecal pellets that sink roughly 10 times faster than bulk oceanic detritus, but their impacts on biogeochemical cycles in the ocean interior are poorly understood. Using a coupled physical-biogeochemical model, we find that fast-sinking detritus decreased global net primary production and surface export, but increased deep sequestration and transfer efficiency in much of the extratropics and upwelling zones. Fast-sinking detritus generally decreased total suboxic and hypoxic volumes, reducing a "large oxygen minimum zone (OMZ)" bias common in global biogeochemical models. Newly aerobic regions at OMZ edges exhibited reduced transfer efficiencies in contrast with global tendencies. Reductions in water column denitrification resulting from improved OMZs improved simulated nitrate deficits relative to phosphate. The carbon flux to the benthos increased by 11% with fast-sinking detritus from fishes and pelagic tunicates, yet simulated benthic fluxes remained on the lower end of observation-based estimates.

Plain Language Summary

Marine ecosystems play a critical role in the global carbon cycle through the food web regulation of air-sea carbon fluxes and the transfer of particulate matter from the upper oceans to depth. Recent evidence has suggested that the detritus from fishes and gelatinous zooplankton (GZ), specifically the pelagic tunicates such as salps and pyrosomes, may have a disproportionate impact on the ocean's biological pump due to them sinking approximately 10x faster than bulk detritus. These fluxes result in increased sequestration of particulate carbon and nutrients into the deep oceans, but their impact on biogeochemical cycles at depth is poorly understood. Here, we investigated the sensitivity of deep ocean carbon, oxygen, and nutrient cycles to fast-sinking detritus from tunicates and fishes. We found that the fast-sinking detritus decreased surface productivity and export, as well as the size of ocean oxygen minimum zones (OMZs). Also, we examined whether observational evidence of seafloor oxygen consumption could support the increased detrital fluxes (and respiration) at depth, and found that even with the increased oxygen consumption, the modeled values were still below the observations. This suggests that these processes could be realistically incorporated into future generations of Earth System Models.

1. Introduction

In the ocean's biological carbon pump, carbon dioxide (CO_2) is fixed in the surface oceans by algal photosynthesis, and particulate carbon sinks from the surface to depth and regulates the vertical gradient of carbon and nutrients in the ocean (Sarmiento & Gruber, 2006). The strength of this pump is measured by not only how much particulate organic carbon (POC) it exports from the surface oceans (between 4-10 Pg C y^{-1}; DeVries & Weber, 2017; Dunne et al., 2007; Henson et al., 2011), but also how efficiently that exported material sinks to the deep sea (i.e., transfer efficiency or T_{eff}; Francois et al., 2002; Wilson et al., 2022). A range of factors influence T_{eff}: the presence of ballast materials (Armstrong et al., 2002), temperature and oxygen-dependent remineralization (Cram et al., 2018; Marsay et al., 2015), and phytoplankton size structure (Weber et al., 2016). While this understanding is largely based on sediment trap observations (e.g., Armstrong et al., 2002; Martin et al., 1987), a less commonly considered factor is the presence of fast-sinking carcasses (jelly-falls) and/or fecal pellets from gelatinous zooplankton and fishes, which are not well captured in the sediment record.

Gelatinous zooplankton (GZ), and in particular, pelagic tunicates (salps, pyrosomes), are notable for their extremely fast-sinking fecal pellets and carcasses, which can exceed 1500 m d^{-1} (Bruland & Silver, 1981; Caron et al., 1989; Lebrato, Mendes, et al., 2013) and result in mass depositions on the seafloor (Henschke et al., 2013; Lebrato, Molinero, et al., 2013; Lebrato & Jones, 2009). Similarly, the fecal pellets of marine fishes can also sink quickly, as the few studies that have measured them show average sinking speeds of 750-1100 m d^{-1} (Robison & Bailey, 1981; Saba & Steinberg, 2012; Staresinic et al., 1983). This is in contrast to marine snow, phytoplankton aggregates, and small crustacean zooplankton (e.g., copepod) fecal pellets that sink at *ca.* 30-300 m d^{-1} (Turner, 2015). Accordingly, several modeling studies have investigated the impact of fast-sinking GZ-mediated POC on T_{eff} (Clerc et al., 2023; Lebrato et al., 2019; Luo et al., 2020), yet none have investigated the combined effect of GZ and fishes, nor more importantly, the impact of these fast-sinking detritus on biogeochemical cycles in the deep ocean.

In addition to direct estimates of detrital flux (sediment traps, Thorium-234 isotopes; Buesseler et al., 2020), the oxygen and macronutrient (e.g., nitrate) concentrations deep in the water column and at the seafloor can also constrain estimates of the biological pump (Andersson et al., 2004; Sulpis et al., 2023). Organic matter remineralization consumes oxygen, but slows significantly in oxygen minimum zones (OMZs) as oxygen is depleted and anaerobic processes, such as denitrification, dominate (Devol & Hartnett, 2001; Van Mooy et al., 2002; Weber & Bianchi, 2020). Unfortunately, the representation of OMZs in coarse-resolution global models has historically been a challenge, with models generally overestimating the extent and misrepresenting the change in OMZs relative to observations (Cabré et al., 2015; Oschlies et al., 2018; Stramma et al., 2012). While these discrepancies have been attributed in part to weak ventilation and poorly resolved equatorial currents (e.g., Busecke et al., 2019; Duteil et al., 2014), other factors such as the stoichiometry of exported organic matter (Devries & Deutsch, 2014; Moreno et al., 2018), and the representation of zooplankton vertical migration (Bianchi et al., 2013) and associated zooplankton-particle interactions (Cavan et al., 2017; Cram et al., 2022) may also influence models' ability to represent observed ocean oxygen patterns. It is unknown, however, whether the inclusion of fast-sinking detritus will exacerbate or alleviate model biases in the OMZs.

In this study, we investigate the effects of fast-sinking detritus from tunicates, fishes, and both on biogeochemical cycling using perturbation experiments with a coupled ice-ocean-biogeochemistry model. We assess their impacts on the horizontal and vertical distribution of POC and oxygen in the mesopelagic and deep sea, and quantitatively attribute the fraction of oxygen consumption in the deep sea arising from fast-sinking detritus.

2. Methods

2.1 Fast-sinking detritus flux

We introduced a new, fast-sinking detritus (1000 m d^{-1}) to the GZ-COBALT model. GZ-COBALT (Luo et al., 2022) incorporated two new (gelatinous) zooplankton groups into the COBALTv2 model (Stock et al., 2020): small and large pelagic tunicates, representing appendicularians and thaliaceans (salps, doliolids, pyrosomes), respectively, with all detritus sinking at the bulk detritus rate (100 m d^{-1}). The other marine ecosystem components (heterotrophic bacteria, small and large phytoplankton, diazotrophs, small, medium, and large zooplankton) remain unchanged. Both pelagic tunicate groups are microphageous generalists, able to consume phytoplankton, bacteria, and heterotrophic nanoflagellates, but preferring smaller sized prey. They are predated upon by mesozooplankton and the unresolved higher trophic-level predators. The higher trophic-level predators, which also predate upon the two mesozooplankton classes, serves as a density-dependent loss for zooplankton (Steele & Henderson, 1992). This provides an estimate of the carbon flux from plankton to epipelagic fishes shown to be consistent with observed cross-ecosystem patterns in fisheries catch (Stock et al., 2017). However, this class excludes mesopelagic fishes, which are not represented in our model, despite potentially comprising significant biomass (Irigoien et al., 2014; Proud et al., 2019). Thus, we will henceforth refer to this group as ‘fish’ and utilize the flux to provide a first-order assessment of epipelagic fish.

Detritus in GZ-COBALT is produced from a range of phytoplankton, zooplankton, and fish sources, including phytoplankton aggregation and zooplankton/fish egestion. The fraction of zooplankton egestion going to sinking detritus ranges from 16.7% for microzooplankton to 100% for large mesozooplankton; the rest is partitioned to various dissolved organic matter pools (Stock et al., 2020). Fish and tunicates also generate detritus from 100% of their egestion (fecal pellets), but for fish their egestion fraction is a fixed 35% of ingestion, whereas for tunicates it varies from 20-75% as a function of prey concentration, due to their unique feeding ecology (Harbison et al., 1986; Lombard et al., 2011; Luo et al., 2022). An additional source of tunicate detritus are jelly-falls, which is a mortality that is triggered when ingestion drops below 10% of maximum ingestion rate. Here, only the detritus from large tunicates (thaliaceans) were configured for fast-sinking: 100% of jelly-falls and 75% of egestion. The other 25% of large tunicate egestion is assumed to always sink more slowly (100 m d^{-1}) and represents a combination of pyrosome fecal pellets (Drits et al., 1992) and slow sinking salp and doliolid fecal pellets (Deibel, 1990; Iversen et al., 2017; Patonai et al., 2011; Yoon et al., 2001). For fish, all detritus were fast-sinking (Saba et al., 2021; Saba & Steinberg, 2012; Staresinic et al., 1983).

COBALTv2 utilizes seven prognostic tracers to track the various components of detritus: nitrogen (N), phosphorus (P), silica (Si), iron (Fe), lithogenic dust, calcite, and aragonite (Stock et al., 2020). Carbon is associated with detrital N following the Redfield ratio (106:16). COBALTv2 detritus is assumed to sink at 100 m d^{-1} and undergoes temperature- and oxygen-

dependent remineralization (Laufkötter et al., 2017). Remineralization is inhibited by the presence of ballast materials such as Si, dust, and calcium carbonate (Armstrong et al., 2002; Klaas & Archer, 2002), as well as above 150 m to account for euphotic zone bacterial colonization (Laufkötter et al., 2017; Mislan et al., 2014). Sinking detritus that reaches the seafloor is subject to remineralization or burial following the parameterization of Dunne et al. (2007), with a ramp down function to reduce burial in nearshore areas. Further dynamics from the simple sediment layer are described in the COBALTv2 documentation (Stock et al., 2020).

For fast-sinking detritus, we implemented three new prognostic tracers (for a total of 38) to track fast-sinking N, P, and Fe, which are assumed to sink at 1000 m d^{-1}. This sinking rate represents an approximate median characteristic velocity of salp, pyrosome, and fish fast-sinking detritus (Bruland & Silver, 1981; Caron et al., 1989; Lebrato, Mendes, et al., 2013; Phillips et al., 2009; Saba & Steinberg, 2012; Staresinic et al., 1983; Steinberg et al., 2022). The fast-sinking detritus is also subject to the same temperature- and oxygen-dependent remineralization as the slow sinkers, but not the remineralization inhibiting effects of ballasting nor colonization.

2.2 Experiments

GZ-COBALT with fast POC was run in a global ocean-ice configuration using the Modular Ocean Model 6 (MOM6) and Sea Ice Simulator 2 (SIS2) at a nominal 0.5° horizontal resolution (Adcroft et al., 2019). The model was forced using the 60-year Common Ocean-Ice Reference Experiment II (CORE-II) dataset (Large & Yeager, 2009) and other forcings and initializations as described in Luo et al. (2022). A control and three perturbation experiments were run for five 60-year cycles, or 300 years:

1) No fast-sinking detritus. All detritus sank at 100 m d^{-1}. (Control simulation)
2) Only tunicate detritus was fast-sinking.
3) Only fish detritus was fast-sinking.
4) Both tunicate and fish detritus were fast-sinking.

In the experiments, no other changes to the model were made. Outputs from the last 20 years of the 5^{th} cycle were computed into a climatological mean for analyses.

2.3 Evaluation

For model evaluation, we used particle flux data from 21 observational sites where either free-floating sediment trap or Marine Snow Catcher data were available, compiled by Dinauer et al. (2022), and oxygen and macronutrient concentrations (NO_3, PO_4) from World Ocean Atlas 18 (Garcia et al., 2019a, 2019b). Modeled sediment oxygen utilization rates (OUR) was computed based on POC flux to the bottom, minus burial flux based on Dunne et al. (2007) and sediment denitrification following Middelburg et al. (1996). This was compared with a new global data product of sediment OUR from Jørgensen et al. (2022; hereafter J22), which was constructed using a regression fit to 798 in-situ benthic measurements.

3. Results

The integration of fast-sinking detritus into GZ-COBALT resulted in an overall decline in net primary production (NPP) and particulate organic carbon (POC) export flux past 100 m relative to the control. NPP decreased 7.8%, 9.5%, and 15%, while export decreased 5.6%, 6.8%, and 11% in the tunicate-only, fish-only, and combined cases, respectively, relative to the GZ-COBALT control (NPP: 52.4 Pg C y^{-1}; export: 6.17 Pg C y^{-1}). Declines in the subtropical gyres were most pronounced as the already limiting surface nutrients redistributed further down in the water column due to the fast-sinking detritus (Fig. 1A). Overall, there was a vertical redistribution of nutrients and detritus, with the tunicate-only and fish-only cases exhibiting similar spatial patterns and magnitudes and the combined case giving values slightly less than the sum of the two others. In the top 100 m, fast-sinking detritus production comprised 6.4%, 8.1%, and 13.9% of the total detritus production in the tunicate-only, fish-only, and combined cases, respectively, but the relative proportion of detritus that was fast-sinking increased with depth.

At the sequestration depth, the fast-sinking detritus increased POC flux past 1000 m by 19%, 21%, and 37% (to 1.01, 1.02, and 1.15 Pg C y^{-1} for tunicate-only, fish-only, and combined, respectively; control: 0.84 Pg C y^{-1}), with large increases in much of the extratropics and in upwelling zones (Fig. 1B). A few areas exhibited large declines in POC flux past 1000 m, such as at the northern equatorial Pacific, the northern Indian ocean, the northern Benguela current, and the Canary current. These are all areas where OMZs reduced in size with fast-sinking detritus (Fig. 1B, Fig. 3A) leading to enhanced remineralization rates under newly aerobic conditions. Both transfer efficiency (T_{eff}) and remineralization length scales between 100 m to 1000 m exhibited similar patterns as the POC flux past 1000m, albeit significantly muted (Fig. S1A, Fig. 1D). In the subtropical gyres, the POC flux at 1000 m with fast-sinking detritus was slightly lower than the control, but transfer efficiency increased, indicating this pattern was primarily driven by differences in surface production. Overall, remineralization length scales increased globally, except for the aforementioned areas near OMZs.

POC flux reaching the seafloor showed broad spatial patterns coherent with those at 100 and 1000m. Globally, there were relatively modest enhancements due to the fast-sinking detritus of 5.6%, 6.3%, and 11% (to 1.33, 1.34, and 1.4 Pg C y^{-1} for tunicate-only, fish-only, and combined, respectively) relative to the control (1.26 Pg C y^{-1}; Fig. 1C). Though, at seafloor depths of 2000 m or deeper, the impact of the fast-sinking detritus was much greater (increases of 36.7%, 39.9%, and 67.2%, respectively, relative to 0.28 Pg C y^{-1} in the control). Due to faster detritus sinking speeds, the relative contribution of coastal zones (200 m or shallower) to global seafloor fluxes decreased, from 59% in the control case to 52% for both tunicate-only and fish-only, and 47% for tunicates and fish combined. This comes as transfer efficiency to the seafloor (T_{eff_btm}) was globally enhanced, with the largest increases in the eastern equatorial Pacific (Fig. S1B).

A comparison of the POC export flux profiles at 21 sites (Dinauer et al., 2022; Fig. S2) shows that overall, the model simulations with fast-sinking detritus fell within range of the observations (Fig. 2). Given that the COBALT flux attenuation dynamics were tuned to many of the same observations (Laufkötter et al., 2017), it is unsurprising that the observational match, in terms of bias, RMSE, and correlation coefficient, was best in the control simulation at most sites, though in many cases the differences were quite small (Fig. S3; 14/17, or 82%, and 11/21, or 52%, of sites had correlation and bias within 5% and 25% of the control, respectively). However, notable exceptions were the MX, VERTEX II, III, and GUAT sites off the western Mexico and

Central American coasts, where more fast-sinking detritus significantly improved the model-observational fit. These sites were generally in areas where anaerobic conditions limited export in the control simulation, but not after adding fast-sinking detritus (Fig. 2, S3).

An assessment of the biogeochemical impacts of fast-sinking detritus showed the OMZs shrunk and deepened relative to the control, particularly in the combined case (Fig. 3A, Fig. S4-7). An evaluation of the total hypoxic ($O_2 \leq 60$ mmol m^{-3}) and suboxic ($O_2 \leq 5$ mmol m^{-3}) volume showed that fast-sinking detritus slowed down the expansion of low oxygen zones following model initialization to WOA, and thus reduced the overexpression of hypoxia and suboxia common in global models (Fig. 3D-E). Hypoxia expansion was reduced in all fast-sinking detritus cases through *ca.* 200 years, though the tunicate-only case accelerated to the control simulation afterwards. This was not the case for the fish-only or combined simulations, which remained at a lower hypoxic volume than the control. All fast-sinking detritus experiments decreased the total suboxic volume, with the tunicates and fish combined simulation decreasing suboxia by approximately 40% globally (Fig. 3E). Accordingly, other biogeochemical processes that occur under low oxygen conditions (e.g., denitrification) were also reduced. In the eastern equatorial Pacific, the nitrate deficit in the mesopelagic was much reduced relative to the control (Fig. 3B) and more consistent with observations, as can be seen through the N* field, which is a metric of the excess nitrate over phosphate (Gruber & Sarmiento, 1997). In the abyssal zone (>3km deep), the high transfer efficiency of fast-sinking detritus increased nitrate and decreased oxygen, resulting in modest biases in each. Nonetheless, in a zonal slice of the eastern Pacific following the P18 line, model skill metrics for NO_3, N*, and to a lesser degree, O_2, improved with the addition of fast-sinking detritus (Fig. S4-7).

The increased supply of POC to the seafloor resulted in increases in benthic oxygen consumption of 6.5%, 7.1%, and 12% (to 110, 111, and 116 Tmol O_2 y^{-1} for tunicate-only, fish-only, and combined) relative to the control (103 Tmol O_2 y^{-1}). Even still, values are far lower than the J22 data product, which predicts benthic oxygen utilization rates (OUR) from a linear relationship between NPP and seafloor depth (Fig. 4). This relationship, which was derived from sparse observations, suggests a mean OUR of 1.74 mmol O_2 m^{-2} d^{-1}, which totals approximately 225 Tmol O_2 y^{-1} globally (given a seafloor area of 3.54E14 m^2). While J22 did not publish a total range, an estimated range (roughly derived from their 95% CIs) is ~120-430 Tmol O_2 y^{-1} globally. In the combined case, the modeled OUR in the extratropics and upwelling zones approaches the J22 mean, but values in the subtropics from all models were still significantly lower. However, the simulated global OUR in the fast-sinking detritus cases does approach the J22 lower range.

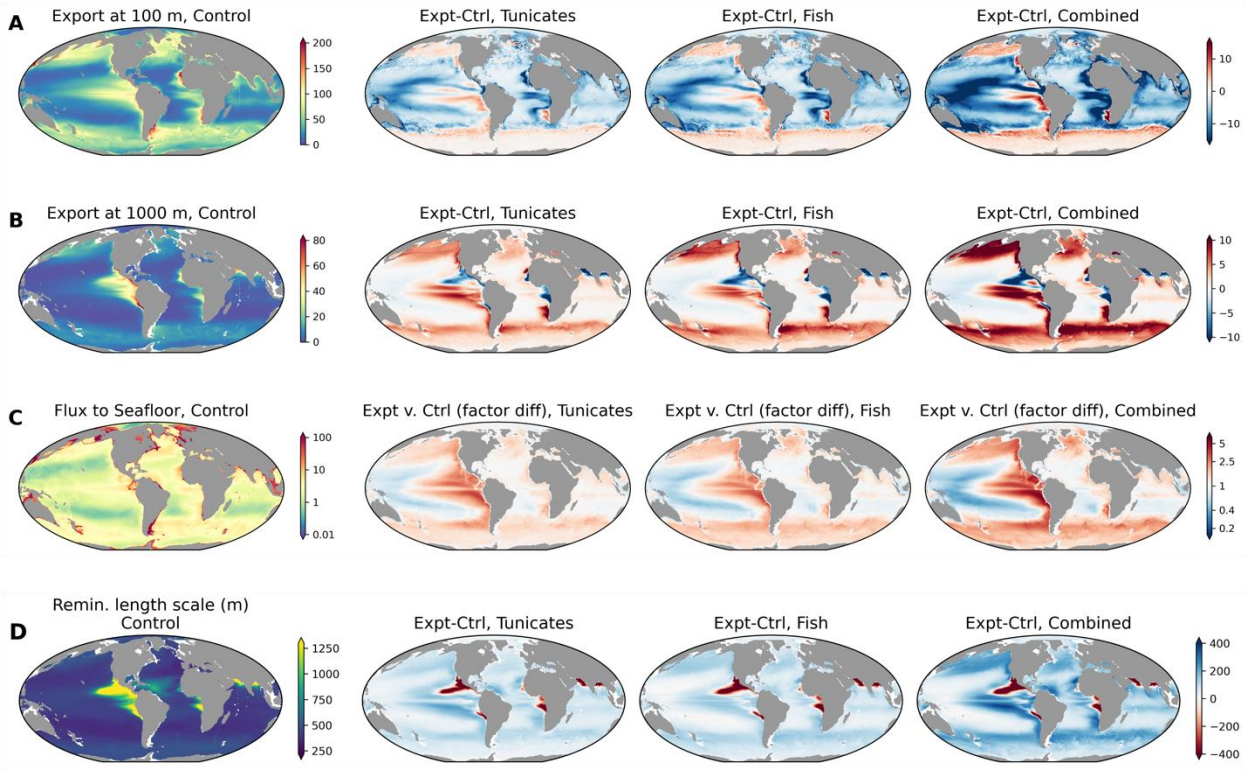

Figure 1. Detrital carbon fluxes and remineralization. (A) Particulate organic carbon (POC) export at 100 m (mg C m^{-2} d^{-1}), showing (left) raw values from the GZ-COBALT control (center to right) the differences between the control and experiments. (B) Same as (A) but at 1000 m. (C) Same as (A) but at the seafloor; note the non-linear colorbars and the use of factor differences. (D) Average remineralization length scale between 100-1000 m, calculated as r = (1000-100) / ln($export_{100}$/$export_{1000}$), where $export_n$ refers to the POC export flux at *n* depth. Colorbars are restricted for display purposes. In the Eastern Tropical North Pacific (ETNP) between 12-18° N and 92-112° W, the remineralization length scales were 2240 m, 1748 m, 1611 m, and 1416 m for the control, tunicates only, fish only, and combined experiments, respectively. These are associated with transfer efficiencies of 65%, 59%, 57%, and 52%, respectively.

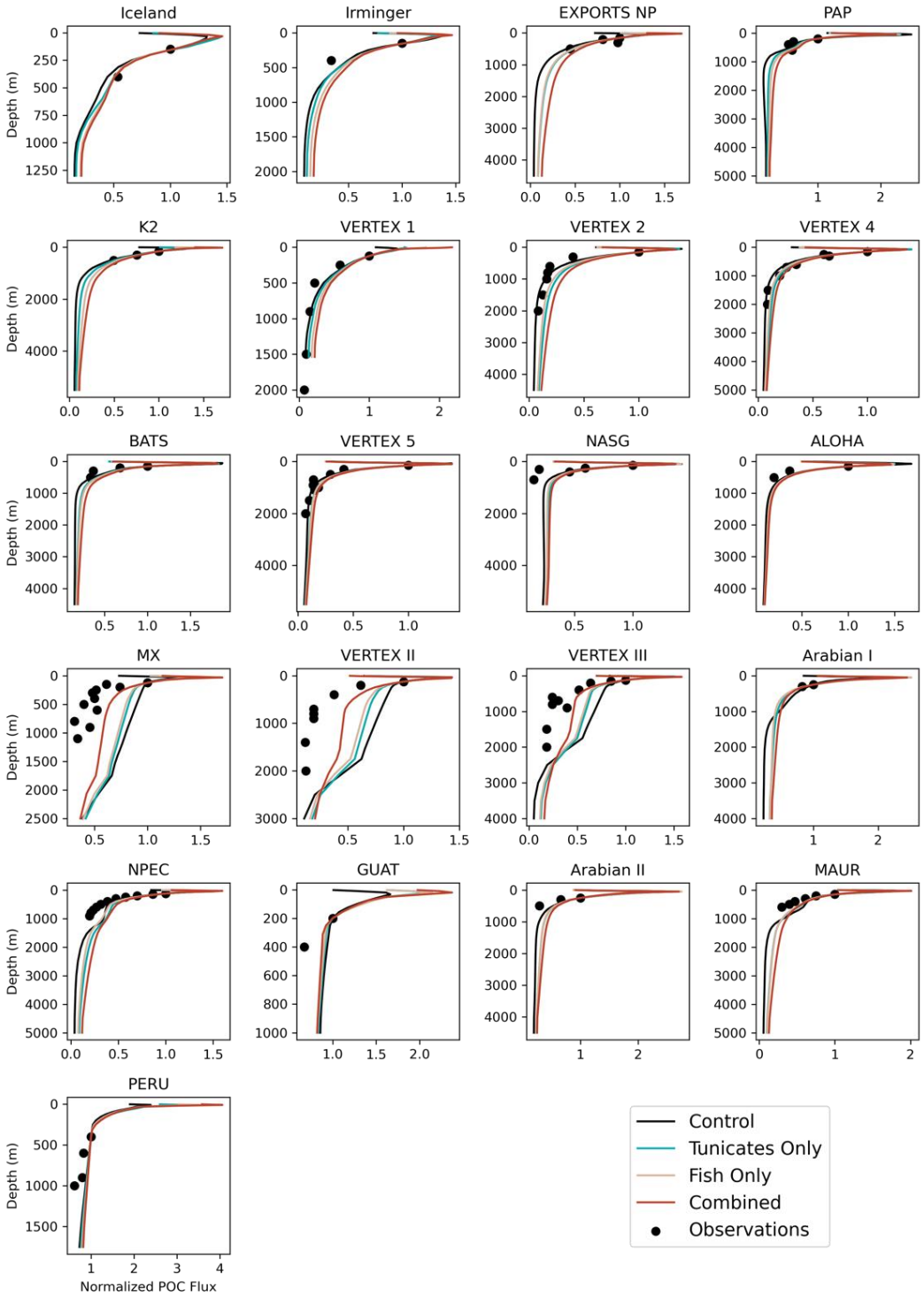

Figure 2. Normalized POC export flux at 22 sites (see Fig. S2), comparing the GZ-COBALT control and the three fast-sinking POC simulations with a set of compiled observations of POC flux profiles from either free-drifting sediment traps or with Marine Snow Catchers (Dinauer et al., 2022). Given the seasonal difference in POC flux profiles, model results from only the season, or a 3-month period, in which the observations were obtained were plotted. Comparison statistics are given in Fig. S3.

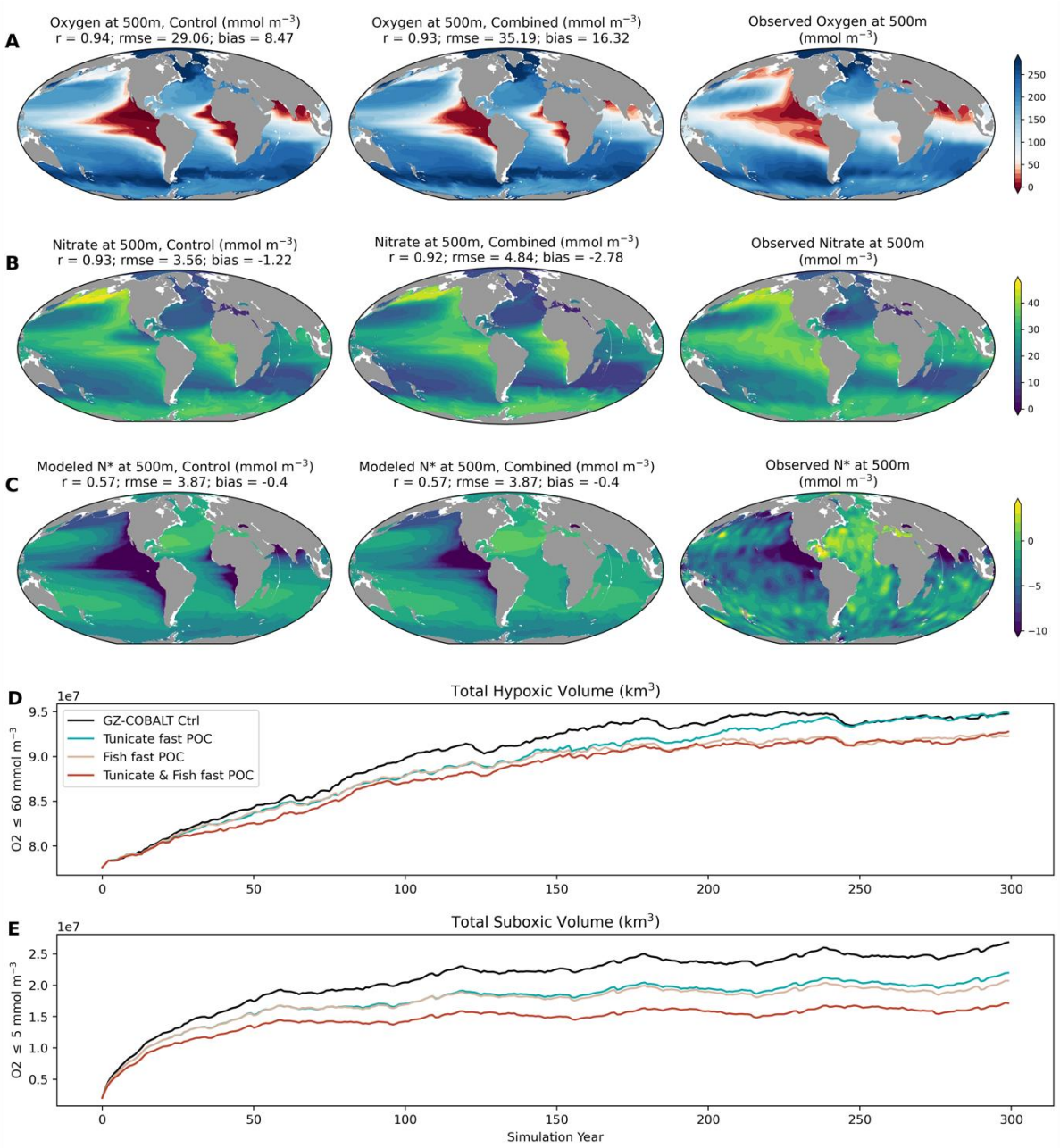

Figure 3. Ocean biogeochemical impacts of fast-sinking detritus. Comparisons of (A) oxygen concentrations (mmol O_2 m^{-3}), (B) nitrate concentrations (mmol NO_3 m^{-3}), and (C) N* (NO_3 – 16*PO_4; mmol m^{-3}) at 500 m depth between the GZ-COBALT control, the tunicates and fish combined case, and observations from the World Ocean Atlas (WOA). Total (D) hypoxic ($O_2 \leq$ 60 mmol m^{-3}) and (E) suboxic ($O_2 \leq 5$ mmol m^{-3}) ocean volume (in km^3) by simulation year, shown for the GZ-COBALT control and all three fast-sinking detritus cases. Note that simulations were initialized from WOA, so the size of the departure from the initial condition in panels (D) and (E) is proportional to the model bias.

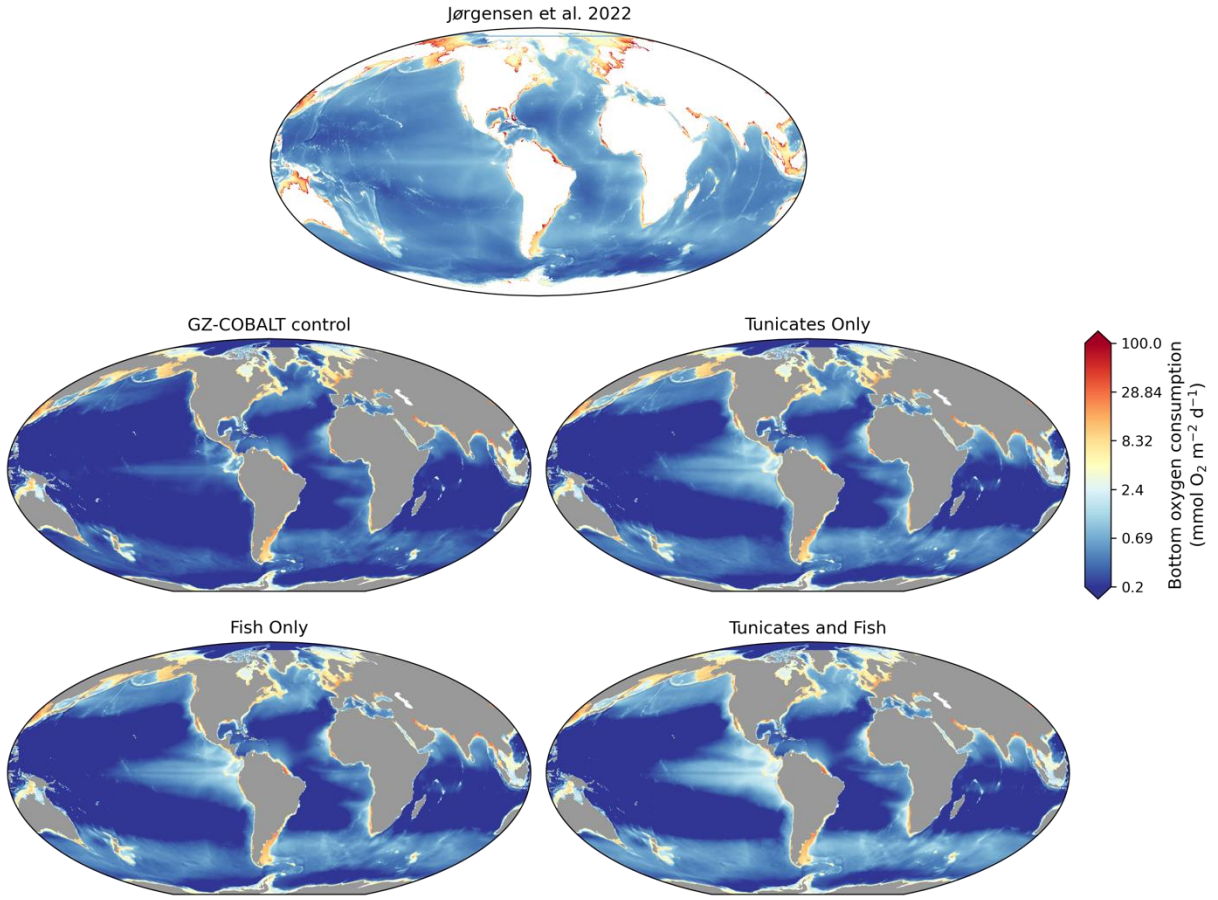

Figure 4. Benthic oxygen utilization. Comparisons between the Jørgensen et al. (2022) observational product (top) and simulated oxygen consumption at the ocean bottom in the GZ-COBALT control and three experimental cases (tunicate-only, fish only, and tunicates and fish combined).

4. Discussion

We used a coupled ocean physical-biogeochemical model to assess the biogeochemical fingerprints of fast-sinking detritus from both pelagic tunicates (e.g., salps, pyrosomes) and fishes in a series of perturbation experiments. The different fast-sinking detritus cases showed that the tunicates-only and fish-only cases were roughly similar in magnitude and spatial extent, with the latter slightly higher along the coasts and in the high productivity regions than the former, consistent with the large scale contrast between tunicates and mesozooplankton in Luo et al. (2022).

Overall, addition of fast-sinking detritus decreased global NPP from 52 to 44-48 Pg C y^{-1}, due to the redistribution of ocean nutrients (N, P) from the upper ocean to depth. Accordingly, POC export at 100 m also declined (from 6.2 to 5.5-5.8 Pg C y^{-1}; Fig. 1A), despite increases in the export ratio. While these declines yielded values still within their range of uncertainty (Carr et al., 2006; Dunne et al., 2007; Field et al., 1998), our results highlight that the processes of generating additional and/or fast-sinking ocean detritus reduces euphotic zone productivity, at least on multi-centennial timescales. Compared to a model that adjusted for the surface impacts of some fast-sinking detritus (e.g., Clerc et al., 2023), our results show a much greater decline in surface export flux. This suggests that recalibration of the bulk POC remineralization scheme (Laufkötter et al., 2017) may be necessary to integrate the full spectrum of sinking detritus into an Earth System Model (ESM).

Accordingly, model skill in representing normalized export fluxes from observations (Dinauer et al., 2022) were slightly degraded, consistent with modifying a component of a tuned model (Laufkötter et al., 2017). Still, there were notable areas in which normalized export fluxes with fast-sinking detritus were a better match for observations than the control, primarily within eastern boundary currents and in OMZs (Fig. 2, S3). This arises due to the interactive effect of fast-sinking detritus on oxygen and remineralization rates. The total remineralization occurring within a given water volume within the mesopelagic decreases due to fast-sinking detritus, and oxygen increases accordingly (Fig. 3). This results in less anaerobic and more aerobic remineralization. Since aerobic remineralization rates are faster, the remineralization length scales are decreased (Fig. 1D). In COBALT, temperature- and oxygen-dependent aerobic remineralization occurs until oxygen reaches a minimum, 0.8 μmol kg^{-1}, below which anaerobic remineralization occurs at 1/10 the aerobic rate (Laufkötter et al., 2017; Stock et al., 2020). This results in a threshold effect and remineralization length scales within OMZs to be up to 10 times longer than in oxygenated waters (Fig. 1D). In the control simulation, the average mesopelagic remineralization length scale in the Eastern Tropical North Pacific (ETNP) was 2240 m, compared to 1416 m in the fish and tunicates combined case. While there is evidence of long remineralization length scales and high transfer efficiencies in the ETNP, the observations instead support remineralization length scales between 800-1650 m (Devol & Hartnett, 2001; Van Mooy et al., 2002), favoring the simulations with fast-sinking detritus (Fig. 2).

Biases in the modeled OMZs have often been attributed to sluggish ventilation and under-resolved equatorial currents in coarse-resolution models (Busecke et al., 2019; Duteil et al., 2014; Getzlaff & Dietze, 2013). So far, the evidence regarding zooplankton-mediated effects on OMZs have indicated that they increase OMZ volume, both through diel vertical migration to the upper margins of the OMZs (Bianchi et al., 2013) and via zooplankton-mediated particle disaggregation (Cram et al., 2022). We acknowledge that there are still significant uncertainties in representing the contribution of fast-sinking detritus from tunicates and fish, such as

proportion of detritus that is fast-sinking in both groups (c.f., Iversen et al., 2017) and mineral ballasting in fecal pellets, which is included for the slow-sinking but not fast-sinking detritus in this current formulation. Additionally, we omitted representation of fish carcasses, which may be non-negligible in high productivity areas (Drazen et al., 2012; Higgs et al., 2014), as well as mesopelagic fishes, where there is still substantial uncertainty regarding both overall biomass and metabolic rates governing their contribution to the biological pump (Davison et al., 2013; Irigoien et al., 2014; McMonagle et al., 2023; Proud et al., 2019). Still, the reduction of OMZ volume and associated biases implies an additional, biological mechanism via fast-sinking tunicate and fish detritus for improving OMZ simulation in ocean biogeochemical models.

The reduced expansion of OMZs in the fast-sinking detritus cases was most pronounced in the suboxic (<5 mmol O_2 m^{-3}) rather than hypoxic (<60 mmol O_2 m^{-3}) waters (Fig. 3). This is likely due to the shifting of the OMZs deeper due to abyssal respiration (Fig. S4-7). Accordingly, water column denitrification, the reduction of oxidized nitrogen (here, NO_3) to N_2 under low oxygen conditions, also declined, resulting in improvements in negative NO_3 biases between 500-2000 m (Fig. S4-7). The modeled oxygen patterns are qualitatively consistent with a recent study by Bianchi et al. (2021), which suggests that fish POC comprise an substantive fraction of oxygen utilization below 1000 m. However, in our simulations, fish POC production comprises 0.56-0.73 Pg C y^{-1}, significantly less than the 1.5 and 3.0 Pg C y^{-1} as suggested by Saba et al., (2021) and Bianchi et al. (2021), respectively. Further, contrary to the suggestion that present day ocean deoxygenation (Schmidtko et al., 2017) may be partially masked by declines in fish populations relative to the preindustrial ocean (Bianchi et al., 2021), our results indicate that in a world with significant declines in fish populations, fish detritus would instead be redistributed to be mediated by mesozooplankton instead, which would sink at the slower, "bulk" rate and redistribute nutrients higher in the water column. This would result in an expansion of OMZs, as remineralization would be shifted towards the surface rather than the mesopelagic to abyssal ocean. It is unclear how tunicate populations are likely to respond in the case of significant fish population declines, but as they primarily compete with microzooplankton rather than mesozooplankton (Luo et al., 2022; Stukel et al., 2021), it is unlikely that fast-sinking tunicate detritus could compensate for decreases in fish detritus.

A key difficulty in constraining deep-sea biogeochemical fluxes is the lack of observational data; however, sedimentary oxygen utilization may be used as an independent, large-scale biogeochemical constraint, as the seafloor serves as the terminal sediment trap (Andersson et al., 2004; Dunne et al., 2007; Middelburg, 2019). Past estimates have suggested a large-scale concurrence between organic matter respiration as estimated from water column sediment traps vs. sedimentary oxygen utilization rates (OUR), particularly in the open ocean (Dunne et al., 2007; Jahnke, 1996), but it was not clear *a priori* whether such observations would support increased fluxes to the bottom from fast-sinking detritus. Our results show that recent seafloor OUR observations (Jørgensen et al., 2022; J22) support increased organic matter fluxes from fast-sinking detritus relative to our control simulation. Indeed, even with the highest T_{eff_btm}, modeled seafloor OUR was a factor of 2 lower than J22, though likely within uncertainty bounds. Reasons for this discrepancy (see also Andersson et al., 2004; Sulpis et al., 2023) could include biases in both the observations (uneven sampling and bias towards coasts and high productivity areas) and the models (coastal productivity in a coarse-scale model is biased low despite broad skill in simulating NPP; Stock et al., 2014). The large-scale benthic flux patterns between oligotrophic gyres and high latitudes as seen in J22 are better reproduced in the fast-sinking detritus case, but fluxes in subtropical regions remain low. These differences highlight a

broader need to reconcile pelagic POC export fluxes with benthic sedimentary demands in ESMs, particularly with increasing focus on coastal zones, blue carbon, and other climate mitigation strategies, where sedimentary dynamics may be increasingly important to resolve.

Acknowledgements

We thank Xiao Liu and Fei Da for their suggestions and comments through an internal review, which improved a previous version of this manuscript. JYL acknowledges support from the NOAA Marine Ecosystem Tipping Points Initiative. We declare no conflicts of interest with respect to the results of this paper.

Open Research

All model outputs necessary to reproduce the results in this manuscript are available at Zenodo at https://doi.org/10.5281/zenodo.8431830. Fortran code for the model code modifications are at https://github.com/jessluo/ocean_BGC/tree/gz_COBALT, and the analysis codes are available at https://github.com/jessluo/gz_COBALT_fastPOC_analysis.

References

Adcroft, A., Anderson, W., Balaji, V., Blanton, C., Bushuk, M., Dufour, C. O., et al. (2019). The GFDL Global Ocean and Sea Ice Model OM4.0: Model Description and Simulation Features. *Journal of Advances in Modeling Earth Systems*, *11*(10), 3167–3211. https://doi.org/10.1029/2019MS001726

Andersson, J. H., Wijsman, J. W. M., Herman, P. M. J., Middelburg, J. J., Soetaert, K., & Heip, C. (2004). Respiration patterns in the deep ocean. *Geophysical Research Letters*, *31*(3), L03304. https://doi.org/10.1029/2003GL018756

Armstrong, R. A., Lee, C., Hedges, J. I., Honjo, S., & Wakeham, S. G. (2002). A new, mechanistic model for organic carbon fluxes in the ocean based on the quantitative association of POC with ballast minerals. *Deep-Sea Research Part II: Topical Studies in Oceanography*. https://doi.org/10.1016/S0967-0645(01)00101-1

Bianchi, D., Galbraith, E. D., Carozza, D. A., Mislan, K. A. S., & Stock, C. A. (2013). Intensification of open-ocean oxygen depletion by vertically migrating animals. *Nature Geoscience*, *6*(7), 545–548. https://doi.org/10.1038/ngeo1837

Bianchi, D., Carozza, D. A., Galbraith, E. D., Guiet, J., & DeVries, T. (2021). Estimating global biomass and biogeochemical cycling of marine fish with and without fishing. *Science Advances*, *7*(41), eabd7554. https://doi.org/10.1126/sciadv.abd7554

Bruland, K. W., & Silver, M. W. (1981). Sinking rates of fecal pellets from gelatinous zooplankton (salps, pteropods, doliolids). *Marine Biology*, *63*(3), 295–300.

Buesseler, K. O., Boyd, P. W., Black, E. E., & Siegel, D. A. (2020). Metrics that matter for assessing the ocean biological carbon pump. *Proceedings of the National Academy of Sciences*, *117*(18), 9679–9687. https://doi.org/10.1073/pnas.1918114117

Busecke, J. J. M., Resplandy, L., & Dunne, J. P. (2019). The Equatorial Undercurrent and the Oxygen Minimum Zone in the Pacific. *Geophysical Research Letters*, *46*(12), 6716–6725. https://doi.org/10.1029/2019GL082692

Cabré, A., Marinov, I., Bernardello, R., & Bianchi, D. (2015). Oxygen minimum zones in the tropical Pacific across CMIP5 models: mean state differences and climate change trends. *Biogeosciences*, *12*(18), 5429–5454. https://doi.org/10.5194/bg-12-5429-2015

Caron, D. a., Madin, L. P., & Cole, J. J. (1989). Composition and degradation of salp fecal pellets: Implications for vertical flux in oceanic environments. *Journal of Marine Research*, *47*, 829–850. https://doi.org/10.1357/002224089785076118

Carr, M. E., Friedrichs, M. A. M., Schmeltz, M., Noguchi Aita, M., Antoine, D., Arrigo, K. R., et al. (2006). A comparison of global estimates of marine primary production from ocean color. *Deep-Sea Research Part II: Topical Studies in Oceanography*. https://doi.org/10.1016/j.dsr2.2006.01.028

Cavan, E. L., Trimmer, M., Shelley, F., & Sanders, R. (2017). Remineralization of particulate organic carbon in an ocean oxygen minimum zone. *Nature Communications*, *8*(1), 14847. https://doi.org/10.1038/ncomms14847

Clerc, C., Bopp, L., Benedetti, F., Vogt, M., & Aumont, O. (2023). Including filter-feeding gelatinous macrozooplankton in a global marine biogeochemical model: model–data comparison and impact on the ocean carbon cycle. *Biogeosciences*, *20*(4), 869–895. https://doi.org/10.5194/bg-20-869-2023

Cram, J. A., Weber, T., Leung, S. W., McDonnell, A. M. P., Liang, J., & Deutsch, C. (2018). The Role of Particle Size, Ballast, Temperature, and Oxygen in the Sinking Flux to the

Deep Sea. *Global Biogeochemical Cycles*, *32*(5), 858–876. https://doi.org/10.1029/2017GB005710

Cram, J. A., Fuchsman, C. A., Duffy, M. E., Pretty, J. L., Lekanoff, R. M., Neibauer, J. A., et al. (2022). Slow Particle Remineralization, Rather Than Suppressed Disaggregation, Drives Efficient Flux Transfer Through the Eastern Tropical North Pacific Oxygen Deficient Zone. *Global Biogeochemical Cycles*, *36*(1). https://doi.org/10.1029/2021GB007080

Davison, P. C., Checkley, D. M., Koslow, J. A., & Barlow, J. (2013). Carbon export mediated by mesopelagic fishes in the northeast Pacific Ocean. *Progress in Oceanography*, *116*, 14–30. https://doi.org/10.1016/j.pocean.2013.05.013

Deibel, D. (1990). Still-water sinking velocity of fecal material from the pelagic tunicate Dolioletta gegenbauri. *Marine Ecology Progress Series*, *62*, 55–60. https://doi.org/10.3354/meps062055

Devol, A. H., & Hartnett, H. E. (2001). Role of the oxygen-deficient zone in transfer of organic carbon to the deep ocean. *Limnology and Oceanography*, *46*(7), 1684–1690. https://doi.org/10.4319/lo.2001.46.7.1684

Devries, T., & Deutsch, C. (2014). Large-scale variations in the stoichiometry of marine organic matter respiration. *Nature Geoscience*, *7*(12), 890–894. https://doi.org/10.1038/ngeo2300

DeVries, T., & Weber, T. (2017). The export and fate of organic matter in the ocean: New constraints from combining satellite and oceanographic tracer observations. *Global Biogeochemical Cycles*. https://doi.org/10.1002/2016GB005551

Dinauer, A., Laufkötter, C., Doney, S. C., & Joos, F. (2022). What Controls the Large-Scale Efficiency of Carbon Transfer Through the Ocean's Mesopelagic Zone? Insights From a New, Mechanistic Model (MSPACMAM). *Global Biogeochemical Cycles*, *36*(10). https://doi.org/10.1029/2021GB007131

Drazen, J. C., Bailey, D. M., Ruhl, H. A., & Smith, K. L. (2012). The Role of Carrion Supply in the Abundance of Deep-Water Fish off California. *PLoS ONE*, *7*(11), e49332. https://doi.org/10.1371/journal.pone.0049332

Drits, A. V., Arashkevich, E. G., & Semenova, T. N. (1992). *Pyrosoma atlanticum* (Tunicata, Thaliacea): grazing impact on phytoplankton standing stock and role in organic carbon flux. *Journal of Plankton Research*, *14*(6), 799–809. https://doi.org/10.1093/plankt/14.6.799

Dunne, J. P., Sarmiento, J. L., & Gnanadesikan, A. (2007). A synthesis of global particle export from the surface ocean and cycling through the ocean interior and on the seafloor. *Global Biogeochemical Cycles*, *21*(4). https://doi.org/10.1029/2006GB002907

Duteil, O., Schwarzkopf, F. U., Böning, C. W., & Oschlies, A. (2014). Major role of the equatorial current system in setting oxygen levels in the eastern tropical Atlantic Ocean: A high-resolution model study. *Geophysical Research Letters*, *41*(6), 2033–2040. https://doi.org/10.1002/2013GL058888

Field, C. B., Behrenfeld, M. J., Randerson, J. T., & Falkowski, P. (1998). Primary production of the biosphere: Integrating terrestrial and oceanic components. *Science*. https://doi.org/10.1126/science.281.5374.237

Francois, R., Honjo, S., Krishfield, R., & Manganini, S. (2002). Factors controlling the flux of organic carbon to the bathypelagic zone of the ocean. *Global Biogeochemical Cycles*. https://doi.org/10.1029/2001gb001722

Garcia, H. E., Weathers, K. W., Paver, C. R., Smolyar, I. V., Boyer, T. P., Locarnini, R. A., et al. (2019a). *World Ocean Atlas 2018. Vol. 4: Dissolved Inorganic Nutrients (phosphate, nitrate and nitrate+nitrite, silicate)*.

Garcia, H. E., Weathers, K. W., Paver, C. R., Smolyar, I. V., Boyer, T. P., Locarnini, R. A., et al. (2019b). *World Ocean Atlas 2018, Volume 3: Dissolved Oxygen, Apparent Oxygen Utilization, and Dissolved Oxygen Saturation*.

Getzlaff, J., & Dietze, H. (2013). Effects of increased isopycnal diffusivity mimicking the unresolved equatorial intermediate current system in an earth system climate model: MIMICKING THE EICS. *Geophysical Research Letters*, *40*(10), 2166–2170. https://doi.org/10.1002/grl.50419

Gruber, N., & Sarmiento, J. L. (1997). Global patterns of marine nitrogen fixation and denitrification. *Global Biogeochemical Cycles*, *11*(2), 235–266. https://doi.org/10.1029/97GB00077

Harbison, G. R., McAlister, V. L., & Gilmer, R. W. (1986). The Response of the Salp, Pegea confoederata, to High Levels of Particulate Material: Starvation in the Midst of Plenty. *Limnology and Oceanography*, *31*(2), 371–382.

Henschke, N., Bowden, D. A., Everett, J. D., Holmes, S. P., Kloser, R. J., Lee, R. W., & Suthers, I. M. (2013). Salp-falls in the Tasman Sea: a major food input to deep-sea benthos. *Marine Ecology Progress Series*, *491*, 165–175. https://doi.org/10.3354/meps10450

Henson, S. A., Sanders, R., Madsen, E., Morris, P. J., Le Moigne, F., & Quartly, G. D. (2011). A reduced estimate of the strength of the ocean's biological carbon pump. *Geophysical Research Letters*, *38*(4). https://doi.org/10.1029/2011GL046735

Higgs, N. D., Gates, A. R., & Jones, D. O. B. (2014). Fish Food in the Deep Sea: Revisiting the Role of Large Food-Falls. *PLoS ONE*, *9*(5), e96016. https://doi.org/10.1371/journal.pone.0096016

Irigoien, X., Klevjer, T. A., Røstad, A., Martinez, U., Boyra, G., Acuña, J. L., et al. (2014). Large mesopelagic fishes biomass and trophic efficiency in the open ocean. *Nature Communications*, *5*(1), 3271. https://doi.org/10.1038/ncomms4271

Iversen, M. H., Pakhomov, E. A., Hunt, B. P. V., van der Jagt, H., Wolf-Gladrow, D., & Klaas, C. (2017). Sinkers or floaters? Contribution from salp pellets to the export flux during a large bloom event in the Southern Ocean. *Deep-Sea Research Part II: Topical Studies in Oceanography*, *138*(December 2016), 116–125. https://doi.org/10.1016/j.dsr2.2016.12.004

Jahnke, R. A. (1996). The global ocean flux of particulate organic carbon: Areal distribution and magnitude. *Global Biogeochemical Cycles*, *10*(1), 71–88. https://doi.org/10.1029/95GB03525

Jørgensen, B. B., Wenzhöfer, F., Egger, M., & Glud, R. N. (2022). Sediment oxygen consumption: Role in the global marine carbon cycle. *Earth-Science Reviews*, *228*, 103987. https://doi.org/10.1016/j.earscirev.2022.103987

Klaas, C., & Archer, D. E. (2002). Association of sinking organic matter with various types of mineral ballast in the deep sea: Implications for the rain ratio. *Global Biogeochemical Cycles*, *16*(4), 63-1-63–14. https://doi.org/10.1029/2001GB001765

Large, W. G., & Yeager, S. G. (2009). The global climatology of an interannually varying air - Sea flux data set. *Climate Dynamics*. https://doi.org/10.1007/s00382-008-0441-3

Laufkötter, C., John, J. G., Stock, C. A., & Dunne, J. P. (2017). Temperature and oxygen dependence of the remineralization of organic matter. *Global Biogeochemical Cycles*, *31*(7), 1038–1050. https://doi.org/10.1002/2017GB005643

Lebrato, M., & Jones, D. O. B. (2009). Mass deposition event of Pyrosoma atlanticum carcasses off Ivory Coast (West Africa). *Limnology and Oceanography*, *54*(4), 1197–1209. https://doi.org/10.4319/lo.2009.54.4.1197

Lebrato, M., Mendes, P. D., Steinberg, D. K., Cartes, J. E., Jones, B. M., Birsa, L. M., et al. (2013). Jelly biomass sinking speed reveals a fast carbon export mechanism. *Limnology and Oceanography*, *58*(3), 1113–1122. https://doi.org/10.4319/lo.2013.58.3.1113

Lebrato, M., Molinero, J. C., Cartes, J. E., Lloris, D., Melin, F., & Beni-Casadella, L. (2013). Sinking Jelly-Carbon Unveils Potential Environmental Variability along a Continental Margin. *PLoS ONE*, *8*(12), e82070. doi:10.1371/journal.pone.0082070. https://doi.org/10.1371/journal.pone.0082070

Lebrato, M., Pahlow, M., Frost, J. R., Küter, M., Mendes, P. D. J., Molinero, J. C., & Oschlies, A. (2019). Sinking of Gelatinous Zooplankton Biomass Increases Deep Carbon Transfer Efficiency Globally. *Global Biogeochemical Cycles*, *33*. https://doi.org/10.1029/2019GB006265

Lombard, F., Selander, E., & Kiørboe, T. (2011). Active prey rejection in the filter-feeding appendicularian *Oikopleura dioica*. *Limnology and Oceanography*, *56*(4), 1504–1512. https://doi.org/10.4319/lo.2011.56.4.1504

Luo, J. Y., Condon, R. H., Stock, C. A., Duarte, C. M., Lucas, C. H., Pitt, K. A., & Cowen, R. K. (2020). Gelatinous zooplankton-mediated carbon flows in the global oceans: A data-driven modeling study. *Global Biogeochemical Cycles*. https://doi.org/10.1029/2020GB006704

Luo, J. Y., Stock, C. A., Henschke, N., Dunne, J. P., & O'Brien, T. D. (2022). Global ecological and biogeochemical impacts of pelagic tunicates. *Progress in Oceanography*, *205*, 102822. https://doi.org/10.1016/j.pocean.2022.102822

Marsay, C. M., Sanders, R. J., Henson, S. A., Pabortsava, K., Achterberg, E. P., & Lampitt, R. S. (2015). Attenuation of sinking particulate organic carbon flux through the mesopelagic ocean. *Proceedings of the National Academy of Sciences*, *112*(4), 1089–1094. https://doi.org/10.1073/pnas.1415311112

Martin, J. H., Knauer, G. A., Karl, D. M., & Broenkow, W. W. (1987). VERTEX: carbon cycling in the northeast Pacific. *Deep Sea Research Part A. Oceanographic Research Papers*, *34*(2), 267–285.

McMonagle, H., Llopiz, J. K., Hilborn, R., & Essington, T. E. (2023). High uncertainty in fish bioenergetics impedes precision of fish-mediated carbon transport estimates into the ocean's twilight zone. *Progress in Oceanography*, *217*, 103078. https://doi.org/10.1016/j.pocean.2023.103078

Middelburg, J. J. (2019). *Marine Carbon Biogeochemistry: A Primer for Earth System Scientists*. Cham: Springer International Publishing. https://doi.org/10.1007/978-3-030-10822-9

Middelburg, J. J., Soetaert, K., Herman, P. M. J., & Heip, C. H. R. (1996). Denitrification in marine sediments: A model study. *Global Biogeochemical Cycles*, *10*(4), 661–673. https://doi.org/10.1029/96GB02562

Mislan, K. A. S., Stock, C. A., Dunne, J. P., & Sarmiento, J. L. (2014). Group behavior among model bacteria influences particulate carbon remineralization depths. *Journal of Marine Research*, *72*(3), 183–218. https://doi.org/10.1357/002224014814901985

Moreno, A. R., Hagstrom, G. I., Primeau, F. W., Levin, S. A., & Martiny, A. C. (2018). Marine phytoplankton stoichiometry mediates nonlinear interactions between nutrient supply, temperature, and atmospheric CO₂ *Biogeosciences*, *15*(9), 2761–2779. https://doi.org/10.5194/bg-15-2761-2018

Oschlies, A., Brandt, P., Stramma, L., & Schmidtko, S. (2018). Drivers and mechanisms of ocean deoxygenation. *Nature Geoscience*, *11*(7), 467–473. https://doi.org/10.1038/s41561-018-0152-2

Patonai, K., El-Shaffey, H., & Paffenhofer, G.-A. (2011). Sinking velocities of fecal pellets of doliolids and calanoid copepods. *Journal of Plankton Research*, *33*(7), 1146–1150. https://doi.org/10.1093/plankt/fbr011

Phillips, B., Kremer, P., & Madin, L. P. (2009). Defecation by Salpa thompsoni and its contribution to vertical flux in the Southern Ocean. *Marine Biology*, *156*(3), 455–467. https://doi.org/10.1007/s00227-008-1099-4

Proud, R., Handegard, N. O., Kloser, R. J., Cox, M. J., & Brierley, A. S. (2019). From siphonophores to deep scattering layers: uncertainty ranges for the estimation of global mesopelagic fish biomass. *ICES Journal of Marine Science*, *76*(3), 718–733. https://doi.org/10.1093/icesjms/fsy037

Robison, B. H., & Bailey, T. G. (1981). Sinking rates and dissolution of midwater fish fecal matter. *Marine Biology*, *65*(2), 135–142. https://doi.org/10.1007/BF00397077

Saba, G. K., & Steinberg, D. K. (2012). Abundance, Composition and Sinking Rates of Fish Fecal Pellets in the Santa Barbara Channel. *Scientific Reports*, *2*(1), 716. https://doi.org/10.1038/srep00716

Saba, G. K., Burd, A. B., Dunne, J. P., Hernández-León, S., Martin, A. H., Rose, K. A., et al. (2021). Toward a better understanding of fish-based contribution to ocean carbon flux. *Limnology and Oceanography*, *66*(5), 1639–1664. https://doi.org/10.1002/lno.11709

Sarmiento, J. L., & Gruber, N. (2006). *Ocean biogeochemical dynamics*. Princeton: Princeton University Press.

Schmidtko, S., Stramma, L., & Visbeck, M. (2017). Decline in global oceanic oxygen content during the past five decades. *Nature*, *542*(7641), 335–339. https://doi.org/10.1038/nature21399

Staresinic, N., Farrington, J., Gagosian, R. B., Clifford, C. H., & Hulburt, E. M. (1983). Downward Transport of Particulate Matter in the Peru Coastal Upwelling: Role of the Anchoveta, Engraulis Ringens. In E. Suess & J. Thiede (Eds.), *Coastal Upwelling Its Sediment Record: Part A: Responses of the Sedimentary Regime to Present Coastal Upwelling* (pp. 225–240). Boston, MA: Springer US. https://doi.org/10.1007/978-1-4615-6651-9_12

Steele, J. H., & Henderson, E. W. (1992). The role of predation in plankton models. *Journal of Plankton Research*, *14*(1), 157–172. https://doi.org/10.1093/plankt/14.1.157

Steinberg, D. K., Stamieszkin, K., Maas, A. E., Durkin, C. A., Passow, U., Estapa, M. L., et al. (2022). The outsized role of salps in carbon export in the subarctic Northeast Pacific Ocean. *Global Biogeochemical Cycles*. https://doi.org/10.1029/2022GB007523

Stock, C. A., Dunne, J. P., & John, J. G. (2014). Global-scale carbon and energy flows through the marine planktonic food web: An analysis with a coupled physical–biological model. *Progress in Oceanography*, *120*, 1–28. http://dx.doi.org/10.1016/j.pocean.2013.07.001

Stock, C. A., John, J. G., Rykaczewski, R. R., Asch, R. G., Cheung, W. W. L., Dunne, J. P., et al. (2017). Reconciling fisheries catch and ocean productivity. *Proceedings of the National Academy of Sciences*, 201610238. https://doi.org/10.1073/pnas.1610238114

Stock, C. A., Dunne, J. P., Fan, S., Ginoux, P., John, J., Krasting, J. P., et al. (2020). Ocean Biogeochemistry in GFDL's Earth System Model 4.1 and Its Response to Increasing Atmospheric CO_2. *Journal of Advances in Modeling Earth Systems*, *12*(10). https://doi.org/10.1029/2019MS002043

Stramma, L., Oschlies, A., & Schmidtko, S. (2012). Mismatch between observed and modeled trends in dissolved upper-ocean oxygen over the last 50 yr. *Biogeosciences*, *9*(10), 4045–4057. https://doi.org/10.5194/bg-9-4045-2012

Stukel, M. R., Décima, M., Selph, K. E., & Gutiérrez-Rodríguez, A. (2021). Size-specific grazing and competitive interactions between large salps and protistan grazers. *Limnology and Oceanography*, *66*(6), 2521–2534. https://doi.org/10.1002/lno.11770

Sulpis, O., Trossman, D. S., Holzer, M., Jeansson, E., Lauvset, S. K., & Middelburg, J. J. (2023). Respiration Patterns in the Dark Ocean. *Global Biogeochemical Cycles*, *37*(8), e2023GB007747. https://doi.org/10.1029/2023GB007747

Turner, J. T. (2015). Zooplankton fecal pellets, marine snow, phytodetritus and the ocean's biological pump. *Progress in Oceanography*, *130*, 205–248. https://doi.org/10.1016/j.pocean.2014.08.005

Van Mooy, B. A. S., Keil, R. G., & Devol, A. H. (2002). Impact of suboxia on sinking particulate organic carbon: Enhanced carbon flux and preferential degradation of amino acids via denitrification. *Geochimica et Cosmochimica Acta*, *66*(3), 457–465. https://doi.org/10.1016/S0016-7037(01)00787-6

Weber, T., & Bianchi, D. (2020). Efficient Particle Transfer to Depth in Oxygen Minimum Zones of the Pacific and Indian Oceans. *Frontiers in Earth Science*, *8*, 376. https://doi.org/10.3389/feart.2020.00376

Weber, T., Cram, J. A., Leung, S. W., DeVries, T., & Deutsch, C. (2016). Deep ocean nutrients imply large latitudinal variation in particle transfer efficiency. *Proceedings of the National Academy of Sciences*, *113*(31), 8606–8611. https://doi.org/10.1073/pnas.1604414113

Wilson, J. D., Andrews, O., Katavouta, A., De Melo Viríssimo, F., Death, R. M., Adloff, M., et al. (2022). The biological carbon pump in CMIP6 models: 21st century trends and uncertainties. *Proceedings of the National Academy of Sciences*, *119*(29), e2204369119. https://doi.org/10.1073/pnas.2204369119

Yoon, W., Kim, S., & Han, K. (2001). Morphology and sinking velocities of fecal pellets of copepod, molluscan, euphausiid, and salp taxa in the northeastern tropical Atlantic. *Marine Biology*, *139*(5), 923–928. https://doi.org/10.1007/s002270100630